Rutherford scattering of α-particles from gold foils

Tony Hyun Kim
MIT Department of Physics
(Dated: October 17, 2008)

We perform α-particle scattering off of gold nuclei. The angular dependence of the scattering rate is measured and is shown to be in good agreement ($\chi^2/\text{dof} = 0.93$) with the Rutherford differential cross section, thus validating the concept of the atomic nucleus. The dependence of the rate on the incident energy (at fixed angle) is also considered, providing further verification of the Rutherford formula. ($\chi^2/\text{dof} = 1.45$)

1. INTRODUCTION

By the beginning of the 20th century, the physics community had undertaken an investigation of atomic structure. In particular, the discovery of the electron by J.J. Thomson, the recognition of its subatomic mass, and its detection from various substances all led to the general understanding that this negatively-charged particle was a component of atoms. These advances initiated speculations on the distribution of the compensating positive charge in the overall neutral atom. Of these, the most prominent was the diffuse charge model promoted by Thomson, in which the positive charge is uniformly distributed over the entire volume of the atom.

In this report, we investigate the angular distribution of α-particle scattering off of gold atoms, originally performed in 1909 by Geiger and Marsden under the direction of Rutherford. It is shown that the angular scattering rates are consistent with an atomic model in which the heavy positive charge is assumed to be concentrated at a point, called the *nucleus*, relative to the volume of the atom. Our result strictly contradicts the diffuse charge model, and serves as one of the experimental foundations for the subsequent quantum atomic theory.

As further verification of the Rutherford scattering model, we have also probed the dependence of the scattering rate on the incident α-particle energy. Here, we observe plausible agreement with the Rutherford formula.

2. THEORETICAL BACKGROUND

2.1. Scattering of α-particles from the nucleus

Earlier studies of the electron have shown its mass to be negligible relative to the mass of any atom. It was also known that α-particles were helium ions, which are also much less massive than the typical target atoms used in this experiment. Under the nuclear hypothesis, the essential physics of the scattering experiment is then contained in the Coulombic repulsion of the incident α-particle from a fixed, positive nucleus. (The electrons are too light to deflect α-particles, while the nucleus is too heavy to be deflected by them.) We have then reduced the scattering problem to the well-understood Kepler problem of motion in a $1/r$ potential.

Under the assumption that the target is uniformly illuminated with projectiles, it is possible to derive from the Keplerian orbits the *scattering cross-section*. The cross-section is proportional to the expected scattering rate at an angle θ from the incident direction. As shown in [1], the Rutherford cross-section is:

$$\frac{d\sigma}{d\Omega} = \left(\frac{k}{4E}\right)^2 \cdot \frac{1}{\sin^4(\theta/2)} \tag{1}$$

where $k = \frac{ZZ'e^2}{4\pi\epsilon_0}$ is the appropriate Coulomb factor between the α-particle and the target nucleus; and E is the initial kinetic energy of the incident α-particles.

In contrast to other atomic models that assume a distributed positive charge within the atom, the Rutherford model is remarkable in that it predicts measurably finite scattering rates even at large deflection angles. For instance, the cross-section corresponding to the Thomson model is a rapidly decaying Gaussian, which predicts essentially no scattering beyond a few degrees from gold targets.[2] Hence, the existence of "back-scattering" is crucial in validating the point charge model.

2.2. Energy loss of α-particles in matter

Under the assumption of a heavy, fixed nucleus, the α-particle does no work on the target atom. On the other hand, electrons are easily deflected by the α-particles and therefore absorbs energy from the incident beam.[3] For instance, α-particles can penetrate only about 4cm of air at STP due to this effect.[2]

With the aid of material property tables such as the NIST database[4], it is then possible to perform metrology (calculation of foil thicknesses, etc.) using this phenomenon. In our investigation, we have used this effect primarily to generate beams of lesser energy, in order to probe the energy dependence of the Rutherford cross section (Eq. 1).

3. EXPERIMENTAL SETUP

The main apparatus, consisting of the ^{241}Am α-particle source, the target gold foils, and the detector were arranged inside a vacuum chamber as shown in Fig.

1. Most of our measurements were taken with the vacuum pressure less than 80 microns, where the energy loss suffered by the α-particles through air is negligible.

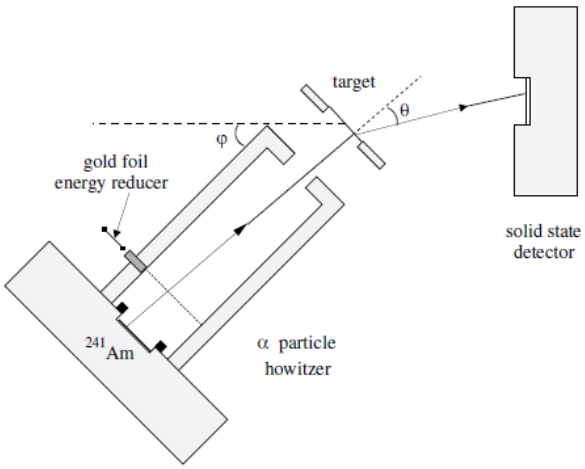

FIG. 1: The α-particle source, the target and the detector inside the vacuum chamber. The detector was fixed in the chamber, while the target holder and the howitzer could be rotated independently. Diagram taken from [2]

The ^{241}Am source provided a 5.486MeV (86%), 5.443MeV (12.7%) α-particle beam. On the side of the barrel, there were slots in which we could place thin foils in order to further reduce the energy of the output beam. The entire howitzer apparatus could be rotated with respect to the detector.

While the vacuum chamber was necessary in order to conduct the experiment, one severe drawback of the setup was that the angular position of the howitzer ϕ was very difficult to assess from outside of the chamber. We estimate our accuracy in setting ϕ to no more than $\pm 1°$.

In addition, the experimental sketch in Fig. 1 highlights complications not accounted for by Eq. 1. Due to the angular spread of the α-particle beam, and the finite sizes of the target and detector, the actual scattering angle θ does not necessarily equal the howitzer angle ϕ. Instead, we expect a howitzer configuration ϕ_0 to yield detection counts corresponding to some spread of angles θ about ϕ_0. In the following section, we will partially correct for this finite geometry effect by convolving the Rutherford cross-section with a "smearing function" that describes the spread of the α-particles from the source.

Finally, the detector output was converted into pulses whose heights corresponded to the energy of the detected particle. These pulses were then recorded by a PC-based MCA. We assume that the MCA channels represent a linear scale for the energy. The scale was constructed using the zero channel for zero energy, in addition to the channel of the dominant 5.486MeV particles. This linear interpretation was assessed by energy loss measurements through foils of known composition and thickness. The result of this calibration is shown in Table I.

TABLE I: Thicknesses of various foils calculated by assuming a linear energy/MCA-channel relationship.

Target foil	Calculated (μm)	Listed (μm) [a]
Au	1.1 ± 0.05	$1.3 \pm .1$
Ti	5.4 ± 1.0	7.6
Ti (Reducer #1)	7.7 ± 1.0	7.6
Ti (Reducer #2)	13.5 ± 0.9	15.8
Fe	8.0 ± 0.7	6.35
Al #1	20.2 ± 1.9	12.7
Al #2	20.0 ± 1.5	12.7

[a] We have less confidence in the correctness of the listed thickness for foils other than gold. While the gold thickness was provided directly by the Junior lab staff, the others were listed on the targets, which looked old and possibly damaged. In addition, there were no uncertainties given on the thicknesses of these other foils.

4. ANALYSIS AND RESULTS

4.1. Identification of valid scattering events

During the experiment, it was clear that the detector was susceptible to environmental factors such as the room lighting. Hence, it was important to have a means of distinguishing the counts actually generated by the scattered α-particles. Fortunately, at low scattering angles ($\theta < 20°$), the count rates were high, and it was possible to clearly distinguish the peak due to the 5.486MeV beam as shown in Fig. 2. We were able to characterize the peak with a Gaussian fit. The final count was then obtained by summing all counts within two standard deviations from the calculated mean.

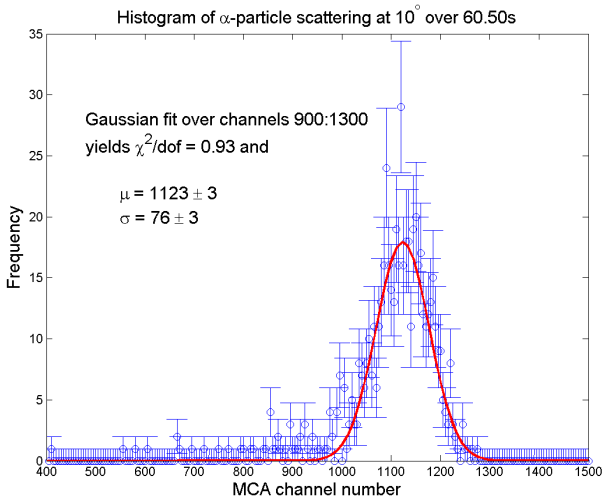

FIG. 2: Result of 10° scattering. For high count rates, the channels of the histogram corresponding to the 5.486MeV incident beam is very apparent.

However, for larger angles, the expected rate of scattering is significantly lower, and it becomes very difficult

to identify the valid scatterers from the baseline level. We resolved this issue by selecting a fixed range of valid channels to be applied to every run. We arrived at a consensus of MCA channels 971 : 1275 after considering many Gaussian fits of data sets displaying obvious peaks. At every angle, we then systematically collected the counts over this fixed interval of MCA channels.

4.2. Angular profile of the α-beam

The sketch of the experimental setup (Fig. 1) shows that the scattering angle θ may not match the howitzer position ϕ exactly. In order to account for this effect, we investigated the angular spread of the α-particle beam by rotating the howitzer about the detector, with no foil in the path. The result is shown in Fig. 3. We note that the angular spreading from the source is quite severe, which betrays the fact the collimator was (inadvertently) not installed during our measurements.

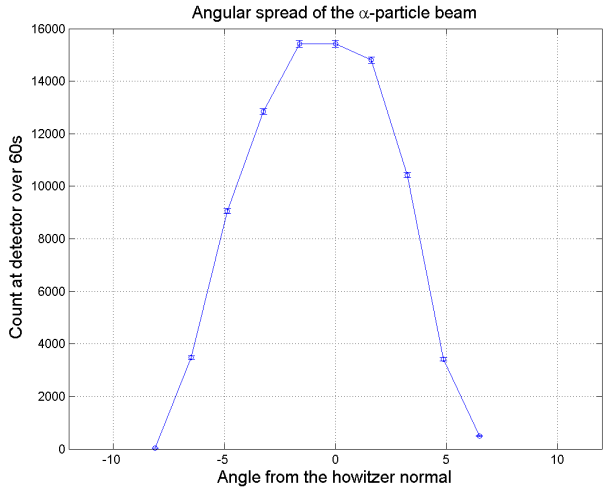

FIG. 3: The α-particle beam shows a broad angular profile. The horizontal axis is to be interpreted as the angle from the direction of the howitzer.

According to Fig. 3, at any fixed howitzer position ϕ_0, α-particles are incident on the foil with angles roughly between $\phi_0 \pm 8°$. It then follows that the scattered angle θ of the particles that reach the detector also lie in this range. In other words, our experiment probes the Rutherford cross-section (Eq. 1) with poor angular resolution. This is modeled mathematically by applying the proper "smearing" function to the cross-section formula.

We have utilized the piecewise linear function $g(\phi - \theta)$ generated from the angular spread measurement (Fig. 3) as the appropriate "smearing function." Then, the expected count rate as a function of the howitzer position is given as a convolution:

$$C(\phi) = C_0 \int_0^{\pi} g(\phi - \theta) \cdot \sin^{-4}(\theta/2) \cdot d\theta \qquad (2)$$

where C_0 is a constant of proportionality, and the $\sin^{-4}(\theta/2)$ factor originates from the underlying Rutherford cross-section. Through this correction, we find dramatic improvements in the theoretical explanation of the measurements. In particular, we expect deviation from the standard Rutherford formula for the smallest angles, since that is the regime for which the scattering rate is most sensitive to small variations in the angle θ.

4.3. Angular dependence of the scattering rate

Based on our fixed-interval counting scheme, the count rates measured at various angles are plotted in Fig. 4. The vertical error bars signify the $\sqrt{N}$ error in the counting process, while the horizontal error bars signify the poor $\pm 1°$ accuracy in our configuring the apparatus. Hence, the effective error (not shown on graph) in the measured rate is $\sigma = \sqrt{N + (d_\phi f)^2 (1°)^2}$ where $f(\phi)$ is the model for the scattering rate. We have modified the fitting procedure to account for errors in both variables.

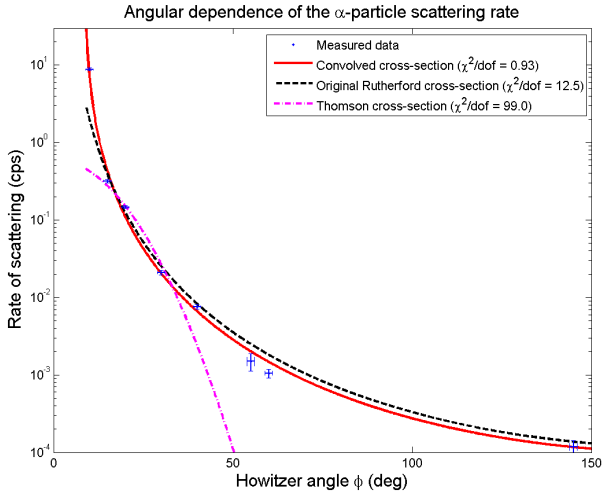

FIG. 4: Scattering rate as a function of howitzer position. Note the significant deviation from the standard Rutherford prediction (dashed line) at 10°. This can be ascribed to the angular spread of the incident beam, since the convolved function (red line) offers striking agreement with this data point. The convolved Gaussian fit yields $C_0 = (1.38 \pm 0.03) \times 10^{-8}$cps in Eq. 2 where g is normalized to unit norm.

Based on the excellent agreement to the modified Rutherford cross-section ($\chi^2/\text{dof} = 0.93$), as well as the 26 instances of back-scattering at 145° (over 2.5 days of observation), we are forced to conclude that the distribution of positive charge within the atom is localized. For comparison, we have also attempted a fit to the Gaussian cross-section arising from the Thomson model, yielding a normalized χ^2 of 99.0. Therefore, our work summarily rejects the diffuse charge model of the atom in favor of the Rutherford hypothesis.

4.4. Energy dependence of the scattering rate

As further investigation of the Rutherford formula (Eq. 1), we have probed for the E^{-2} variation in the scattering rate. With the howitzer angle fixed at $\phi = 20°$, we decreased the energy of the incident beam by inserting reducer foils into the barrel of the howitzer. The modified energies were characterized by striking the detector directly with the reduced beam.

Rather than the fixed-interval counting scheme used in the previous experiment, we were forced to employ a more complicated counting method. The new difficulty was that portions of the reduced-energy beam were clipped by the discriminator of the MCA. It was not feasible to lower the set-point, because electronic noise would then swamp the signal. Therefore, we have chosen to fit and count only the upper-half of each peak. Since we studied relatively small angles, the main peak was quite distinct in each histogram, and could be fitted easily. The half-count was doubled to yield the final count.

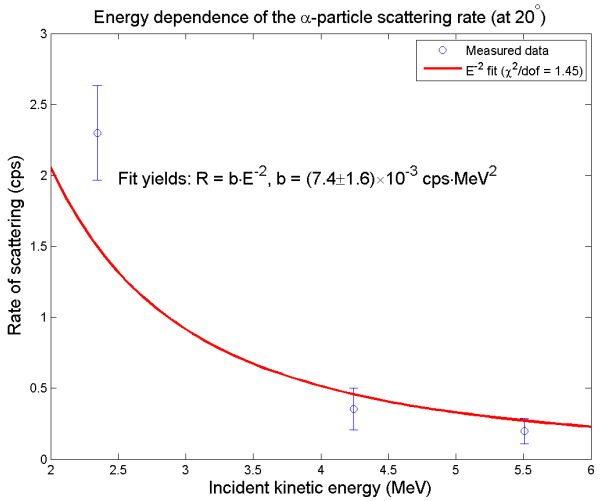

FIG. 5: Scattering rate as a function of incident energy.

In Fig. 5, the major deviation from theory comes from the lowest-energy measurement. Notably, this point had the most severe clipping problem. In any case, the χ^2/dof = 1.45 suggests that the rate vs. energy behavior is real, and that it may be more precisely verified by a better calibrated experiment.

5. ERROR ANALYSIS

Clearly, our experiment was dominated by the ±1° error in setting the howitzer angle. For instance, at 10°, the uncertainty in ϕ contributed 96% of its overall error. The effect was milder for larger angles, with 50% of the error at 60° owing to σ_ϕ. For an improved test of Rutherford scattering, our first suggestion is therefore to improve the angular precision of the howitzer.

Our linear energy interpretation of the MCA channels is also quite suspect. If we take into account the signal pedestal, the reduced beam energies can shift by up to 2%. Moreover, we even suspect that the energy-channel relationship may be nonlinear. In particular, we found that the beam from the ^{241}Am source was beautifully characterized by a double-Gaussian fit, where the second envelope was lower in channel number, and had height 0.14 relative to the main peak. This strongly implies the 5.443MeV portion of the beam. However, the location of the secondary Gaussian contradicted our linear scale. We have attempted an energy scale based on a linear interpolation between the 5.443 and 5.486MeV peaks, but found that the resulting scale predicted foil thicknesses (as in Table I) that were an order of magnitude off of the stated values. Due to these subtleties, we have used the simplest possible interpretation of the MCA channels in our analysis. Ideally, the energy scale should be characterized directly by using calibration sources.

The conclusions drawn from the angular experiment is unaffected by the energy scale, because the intervals were determined empirically to correspond to the main peak.

6. CONCLUSIONS

We performed α-particle scattering from gold foils, and found that the Rutherford cross-section formula gave an excellent fit (χ^2/dof = 0.95) to the scattering rate as a function of angle. In contrast, the Thomson model is utterly incapable of explaining the results. Our measurements therefore reject the diffuse charge model of the atom in favor of the Rutherford hypothesis.

We have also investigated the energy dependence of the scattering rate. Here, despite the shortcomings in our energy calibration, we have found a reasonable agreement with the theoretical predictions (χ^2/dof = 1.45).

[1] H. Goldstein, *Classical Mechanics* (Addison-Wesley, 2002).
[2] J. lab staff, *Rutherford scattering lab guide* (2006).
[3] E. Serge, *Nuclei and Particles* (Benjamin, 1977).
[4] NIST, *Stopping-power and range tables for helium ions*, http://physics.nist.gov/PhysRefData/Star/Text/ASTAR.html.

Acknowledgments

THK gratefully acknowledges Connor McEntee for his partnership in the experiment, as well as Prof. Yamamoto and the Junior lab staff for acquainting us with the apparatus.